Design Strategy for 25% External Quantum Efficiency in Green and Blue Thermally Activated Delayed Fluorescent Devices

*Dong Ryun Lee, Mounggon Kim, Sang Kyu Jeon, Seok-Ho Hwang, Chil Won Lee, and Jun Yeob Lee**

Development of high efficiency organic light-emitting diodes (OLEDs) has been one of key issues of OLEDs because conventional fluorescent OLEDs exhibit low external quantum efficiency (EQE) by nonradiative loss of triplet excitons.[1] This hurdle can be overcome by inducing radiative transition of triplet excitons by singlet-triplet mixing[2] or up-conversion of triplet excitons into singlet excitons.[3] The former process is used for phosphorescent emission and the latter process is utilized for thermally activated delayed fluorescent (TADF) emission. The two methods were proven to be successful to improve the EQE of OLEDs. Especially, the EQE of the phosphorescent OLEDs could reach above 25% in all red, green, and blue devices.[4–7] However, the EQE of the TADF device is still lower than that of phosphorescent OLEDs. In particular, the EQE of blue TADF OLEDs is not in the same level as that of phosphorescent OLEDs although EQE close to 20% has been demonstrated.[8–10]

In general, molecular design of the TADF emitters is the most important factor to develop high efficiency TADF devices. It has been known that the TADF emitters need to be designed to have separated highest occupied molecular orbital (HOMO) and lowest unoccupied molecular orbital (LUMO) for small singlet-triplet energy gap (ΔE_{ST}) and weakly overlapped HOMO and LUMO for efficient light emission.[3] The former condition is desired for up-conversion of triplet excitons into singlet excitons and the latter condition is required for high photoluminescence (PL) quantum yield. Therefore, both conditions should be met to develop highly efficient TADF devices.

Based on this design criteria, various red, green, and blue TADF emitters were synthesized.[8–16] A variety of donor moieties were combined with acceptor moieties via an aromatic linker based on different design strategies. One design approach was to link a donor moiety with an acceptor moiety via a linker[8–15] and the other approach was to link the donor and acceptor moieties without a linker.[16] Typically, the molecular design with the aromatic linker between the donor and acceptor moieties provided high EQE. Additionally, wide dispersion of the HOMO and LUMO in a donor unit was proposed as an effective way of enhancing the quantum efficiency of the blue TADF devices.[8] However, the design strategy in previous work could provide EQE only close to 20%,[8,9] which is inferior to that of phosphorescent OLEDs. Therefore, a new molecular design approach to improve the EQE of the TADF OLEDs is desired.

Herein, we provide a design approach to realize high EQE above 25% in green and blue TADF OLEDs. A molecular design strategy to evenly distribute the HOMO of the TADF emitters over the donor units by introducing the same donor units in the molecular structure as many as possible was successful to reach above 25% EQE in green and blue TADF devices. The design concept was verified by comparing targeted green and blue TADF emitters with control material with uneven HOMO distribution or less donor units.

One green emitter and one blue emitter were prepared as target materials to obtain high EQE in the TADF OLEDs and control materials were compared with the target materials. Diphenyltriazine was an acceptor moiety and carbazole or 3,6-dimethylcarbazole was a donor moiety of the TADF emitters. Two compounds with three donor units in the backbone structure, 9,9′,9″-(5-(4,6-diphenyl-1,3,5-triazin-2-yl)benzene-1,2,3-triyl)tris(9H-carbazole) (TCzTrz) and 9,9′,9″-(5-(4,6-diphenyl-1,3,5-triazin-2-yl)benzene-1,2,3-triyl)tris(3,6-dimethyl-9H-carbazole) (TmCzTrz), were developed as the green and blue TADF emitters for high EQE. To prove the effectiveness of the design strategy to include many donor units, a diphenyltriazine derivative with two carbazole units, 9,9′-(5-(4,6-diphenyl-1,3,5-triazin-2-yl)-1,3-phenylene)bis(9H-carbazole) (DCzTrz), reported in our previous work was assessed as the blue control material with two donor units.[10] Additionally, one diphenyltriazine derivative with one 3,6-dimethylcarbazole and two carbazole units in place of three carbazole or three 3,6-dimethylcarbazole units of TCzTrz and TmCzTrz, 9,9′-(2-(3,6-dimethyl-9H-carbazol-9-yl)-5-(4,6-diphenyl-1,3,5-triazin-2-yl)-1,3-phenylene)bis(9H-carbazole) (DCzmCzTrz), was also prepared to elucidate the necessity of uniform distribution of the HOMO over the entire donor units. The molecular structure of the four TADF emitters used to prove the design approach is shown in **Figure 1**a. The synthetic scheme is depicted in **Scheme 1** and synthetic procedures

---

D. R. Lee, S. K. Jeon, Prof. J. Y. Lee
School of Chemical Engineering
Sungkyunkwan University
2066, Seobu-ro, Jangan-gu, Suwon
Gyeonggi 440-746, South Korea
E-mail: leej17@skku.edu

M. Kim, Prof. S.-H. Hwang, Prof. C. W. Lee
Department of Polymer Science and Engineering
Dankook University
126, Jukjeon-dong, Suji-gu, Yongin
Gyeonggi 448-701, South Korea

DOI: 10.1002/adma.201502053

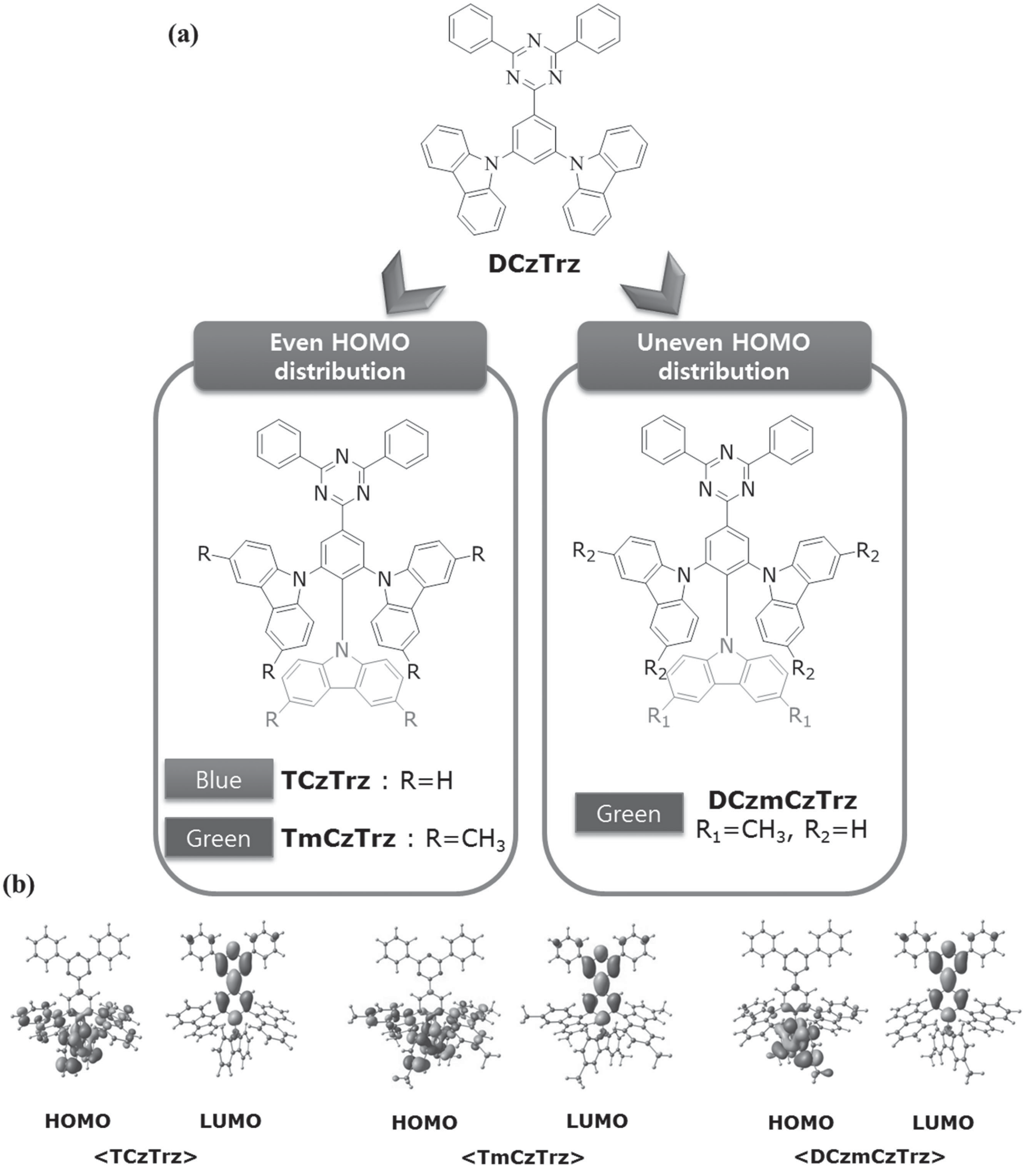

Figure 1. a) Molecular structure of DCzTrz, TCzTrz, TmCzTrz, and DCzmCzTrz. b) HOMO and LUMO distribution of TCzTrz, TmCzTrz, and DCzmCzTrz.

are explained in the Supporting Information in detail. All compounds were prepared by coupling reaction, but two-step coupling reaction was used to synthesize DCzmCzTrz. 3,6-Dimethylcarbazole was coupled with a central F unit of 2,4-diphenyl-6-(3,4,5-trifluorophenyl)-1,3,5-triazine intermediate by controlling molar ratio of 3,6-dimethylcarbazole to 2,4-diphenyl-6-(3,4,5-trifluorophenyl)-1,3,5-triazine because the reactivity of the central F atom is higher than the other F units by the strong electron withdrawing character of two F units surrounding the central F unit.

In order to reach high EQE in the TADF devices, high PL quantum yield of the TADF emitters is essential and it is closely

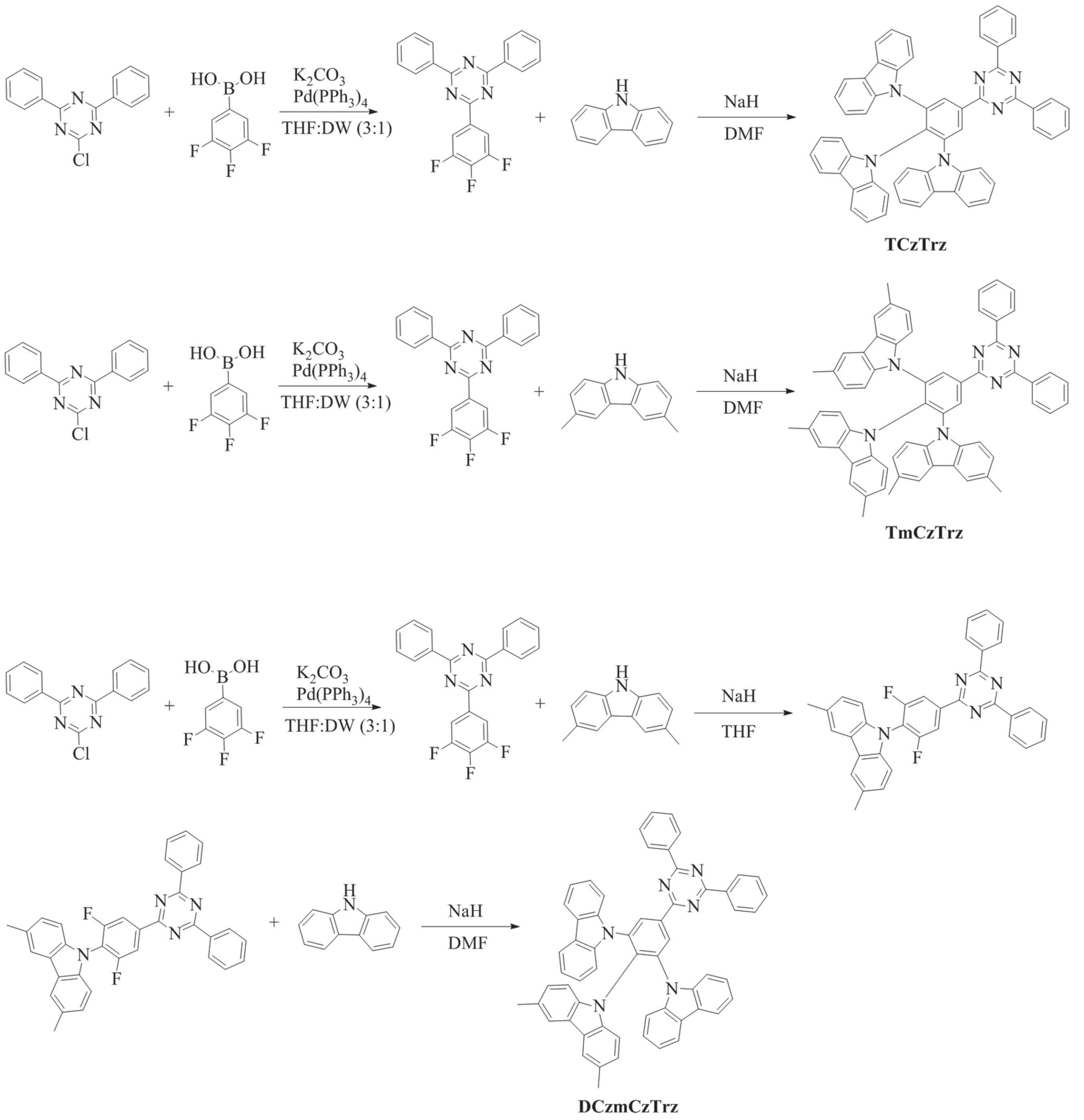

Scheme 1. Synthetic scheme of TCzTrz, TmCzTrz, and DCzmCzTrz.

related with HOMO–LUMO overlap of the TADF emitters and reverse intersystem crossing by up-conversion. Therefore, electronic calculation of the HOMO and LUMO was conducted to study the HOMO–LUMO overlap and photophysical characterization was carried out to extract PL related photophysical parameters. Figure 1b shows electronic calculation results of the TADF emitters which describes the HOMO and LUMO distribution. The HOMO and LUMO were isolated, and small overlap of the HOMO and LUMO was detected in all TADF emitters. Relating the chemical structure of the DCzTrz[10] and TCzTrz TADF emitters with the HOMO distribution, the HOMO was evenly dispersed over all carbazole units incorporated in the molecular structure. Although three carbazole units were attached to the central phenyl ring of TCzTrz, the HOMO dispersion was uniform over all three carbazole units. In addition, the three carbazole units expanded the HOMO to the central phenyl linker extensively, and overlap of the HOMO and LUMO was observed. Detailed calculated parameters are summarized in Table S1, Supporting Information. All three TADF emitters are expected to possess small ΔE_{ST} for TADF behavior.

The chemical structure of TCzTrz, TmCzTrz, and DCzmCzTrz was also correlated with the HOMO and calculated

Table 1. Photophysical properties of DCzTrz, TCzTrz, TmCzTrz, and DCzmCzTrz.

	UV–vis absorption edge [nm]	Singlet energy[a)] [eV]	Triplet energy[b)] [eV]	ΔE_{ST} [eV]	PLQY solution[c)] [%]	PLQY film[d)] [%]	Delayed fluorescence lifetime [μs]
DCzTrz[10]	411	3.09	2.86	0.23	43 (17)	–	31.0
TCzTrz	414	2.96	2.80	0.16	100 (47)	100 (81)	13.5
TmCzTrz	447	2.86	2.79	0.07	99 (39)	100 (86)	13.3
DCzmCzTrz	427	2.93	2.73	0.20	84 (52)	98 (89)	9.7

[a)] Singlet energy was calculated from the onset wavelength of fluorescent emission; [b)]Triplet energy was calculated from the onset wavelength of phosphorescent emission; [c)]PLQY measurement was performed in toluene solution after 10 min of nitrogen bubbling; [d)]PLQY measurement was performed using 30% TADF emitting material doped DPEPO film. Values in parentheses: before nitrogen bubbling.

photophysical parameters. In the case of TCzTrz and TmCzTrz, the HOMO was uniformly distributed over all donor units because the same donor unit was substituted. However, the HOMO of DCzmCzTrz was mostly localized on the 3,6-dimethylcarbazole by relatively strong electron richness of 3,6-dimethylcarbazole compared to carbazole. Nonuniform HOMO distribution was observed in the DCzmCzTrz, while uniform HOMO distribution was observed in the TCzTrz and TmCzTrz. The LUMO of TCzTrz, TmCzTrz, and DCzmCzTrz was similarly dispersed over the diphenyltriazine moiety. The HOMO and LUMO were overlapped in the phenyl linker, which connects the donor and acceptor moieties.

Photoluminescence (PL) quantum yields of DCzTrz, TCzTrz, TmCzTrz, and DCzmCzTrz in toluene measured using an integrating sphere after N_2 bubbling were 43%,[10] 100%, 99%, and 84%, respectively. TCzTrz and TmCzTrz showed almost 100% PL quantum yield under N_2 compared to 47% and 39% in ambient conditions, supporting up-conversion of triplet excitons for radiative transition by reverse intersystem crossing process. From the PL quantum yield data, Φ_{TADF}/Φ_T representing relative up-conversion efficiency of triplet excitons was calculated, where Φ_{TADF} is PL quantum yield of TADF and Φ_T is quantum yield of intersystem crossing from singlet excited state to triplet excited state.[8] The Φ_{TADF} values of TCzTrz, TmCzTrz, and DCzmCzTrz were 53, 60, and 32%, respectively. The Φ_{TADF}/Φ_T values were 100%, 98%, and 67% for TCzTrz, TmCzTrz, and DCzmCzTrz, which indicates that triplet excitons of TCzTrz and TmCzTrz are completely converted into singlet excitons, while only 67% of triplet excitons of DCzmCzTrz are transformed into singlet excitons. This result is due to small ΔE_{ST} of TCzTrz and TmCzTrz, which is presented in **Table 1**. Therefore, TCzTrz and TmCzTrz may be more efficient than DCzmCzTrz to harvest triplet excitons for singlet emission. PL quantum yield of TADF emitters doped in bis[2-(diphenylphosphino)phenyl]ether oxide (DPEPO) host was also measured and the triplet to singlet conversion efficiency was high in the TCzTrz and TmCzTrz. Φ_{TADF} values of TCzTrz, TmCzTrz, and DCzmCzTrz in the DPEPO host were 19%, 14%, and 9%, respectively, and the Φ_{TADF}/Φ_T values 100%, 100%, and 82%. From the PL quantum yields of DCzTrz and TCzTrz, it can be assumed that introduction of three donor units is better than introduction of two donor units for up-conversion of triplet excitons. Similarly, it can be presumed that even HOMO distribution is preferred to uneven HOMO distribution to reach high PL quantum yield and triplet to singlet conversion efficiency from the PL quantum yields of TCzTrz, TmCzTrz, and DCzmCzTrz. PL quantum yields of the three emitting materials are listed in Table 1 in addition to PL quantum yield of DCzTrz.

Basic photophysical parameters were collected from UV–vis and PL measurements, and are summarized in Table 1. UV–vis absorption, room temperature PL and low temperature PL data are presented in Figure S1 in the Supporting Information. Comparing DCzTrz and TCzTrz, additional donor unit lowered the singlet and triplet energy of the TADF emitter by strengthened donating power and extended conjugation structure. Comparing TCzTrz, TmCzTrz, and DCzmCzTrz, relatively strong electron donating character of 3,6-dimethylcarbazole to carbazole lowered the singlet energy of TmCzTrz and DCzmCzTrz. The relatively low singlet energy of TmCzTrz to that of DCzmCzTrz is due to strong electron donating character by three 3,6-dimethylcarbazole units of TmCzTrz compared to one 3,6-dimethylcarbazole unit of DCzmCzTrz. ΔE_{ST} of DCzTrz, TCzTrz, TmCzTrz, and DCzmCzTrz were 0.23, 0.16, 0.07, and 0.20 eV, respectively. From the ΔE_{ST} of DCzTrz and TCzTrz, it can be suggested that the additional donor unit reduces the ΔE_{ST} and increases the PL quantum yield by improved reverse intersystem crossing of the TADF emitters. In the case of TCzTrz and TmCzTrz, the ΔE_{ST} was small in the TmCzTrz because the donor strength of the donors was different.

Transient PL measurement of TCzTrz, TmCzTrz, and DCzmCzTrz was carried out from 100 K to room temperature to monitor delayed fluorescence behavior. Transient PL decay of the three TADF emitters is described in **Figure 2**. The delayed fluorescence component of the three TADF emitters was intensified at high temperature, which proposed that the delayed emission of the three emitters is activated by thermal energy. Excited state lifetimes for delayed emission of TCzTrz, TmCzTrz, and DCzmCzTrz were 13.5, 13.3, and 9.7 μs, respectively. Compared with the lifetime for TADF emission of other triazine and carbazole derived TADF emitters, the lifetime of TCzTrz, TmCzTrz, and DCzmCzTrz was relatively short because of facile up-conversion by small ΔE_{ST}. The small ΔE_{ST} of the three TADF emitters induced efficient up-conversion, short lifetime for TADF and high PL quantum yields. Lifetime for the delayed emission of DCzTrz with two carbazole units was 31.0 μs,[10] which was much longer than that of TCzTrz with three carbazole units. Prompt and delayed emission spectra are shown in Figure S2 in the Supporting Information. Delayed emission spectra of TCzTrz, TmCzTrz, and DCzmCzTrz were almost identical to prompt emission spectra of each TADF emitter,

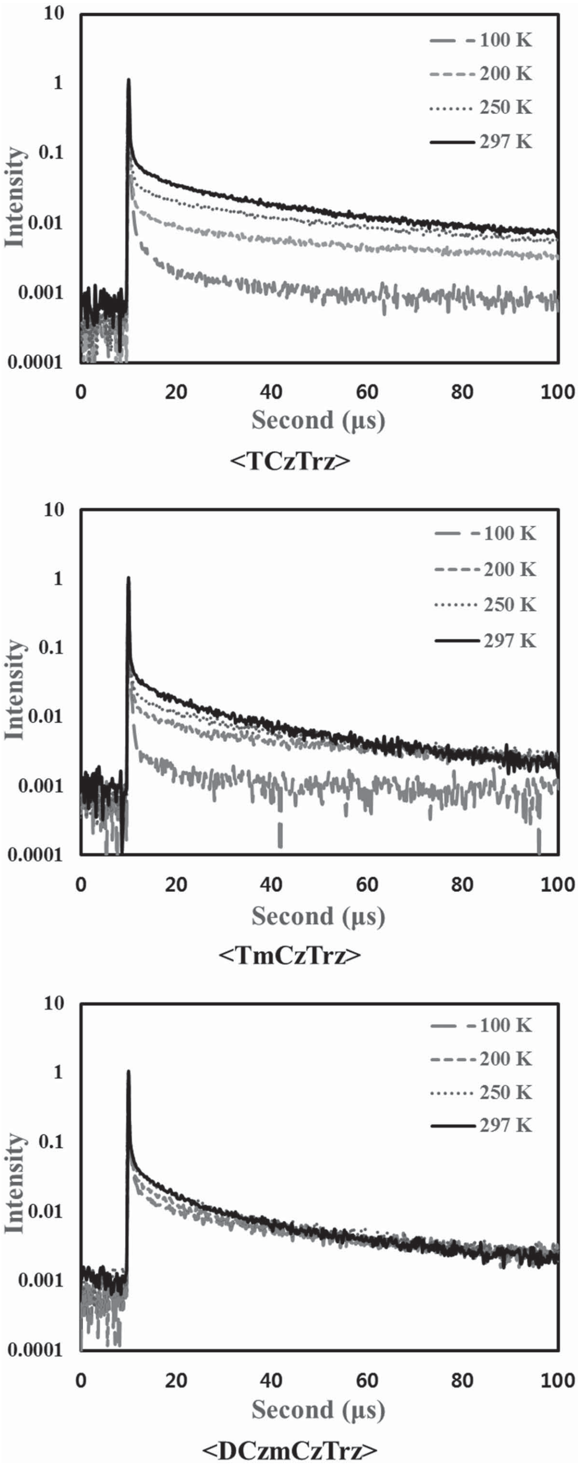

Figure 2. Transient decay curves of TCzTrz, TmCzTrz, and DCzmCzTrz from 100 to 297 K.

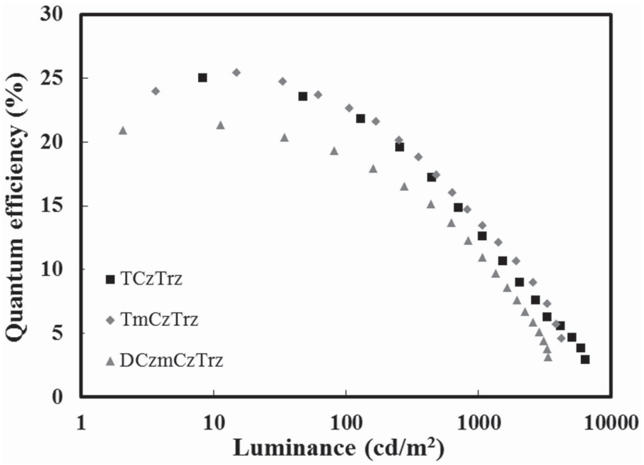

Figure 3. Quantum efficiency-luminance curves of TCzTrz, TmCzTrz, and DCzmCzTrz devices. Doping concentrations of TCzTrz, TmCzTrz, and DCzmCzTrz were 40%, 30%, and 20%, respectively.

which indicates that the delayed emission is caused by TADF process.

Device performances of the TADF emitters were characterized by doping the TADF emitters in a high triplet energy DPEPO host. Hole transport layer structure was optimized for each TADF emitter. EQE of the TADF devices was plotted according to the luminance of the devices in **Figure 3**. Current density and luminance data are presented in the Supporting information (Figure S3). EQE of the TADF devices was calculated based on the assumption that light emission profile follows Lambertian distribution after confirming that angle dependent radiation intensity of the devices agrees with Lambertian emission pattern (Figure S4, Supporting Information). Correlating the number of donor units with the EQE, the increase of the number of donor units enhanced the EQE. Maximum EQE of the TCzTrz and DCzTrz devices were 25.0% and 17.8%,[10] respectively. A dramatic improvement of the EQE was realized by increasing the number of carbazole units attached to the central phenyl linker. The EQE of 25.0% of the TCzTrz blue device is higher than 20.6% of the state of the art EQE of the blue TADF device reported by Adachi and coworkers.[8] More than 20% improvement in the EQE was made by adopting a molecular design with three carbazole units. Comparing TCzTrz, TmCzTrz, and DCzmCzTrz devices, the EQE was in the order of TCzTrz (25.0%) ≈ TmCzTrz (25.5%) > DCzmCzTrz (21.3%). Although the DCzmCzTrz device with one 3,6-dimethylcarbazole and two carbazole units exhibited high EQE, the TCzTrz and TmCzTrz device worked better than the DCzmCzTrz device. Both green TmCzTrz and blue TCzTrz devices showed high quantum efficiency above 25%. The better EQE of the TCzTrz and TmCzTrz devices than that of DCzmCzTrz device can be correlated with the PL quantum yield of the three emitters. In particular, the triplet to singlet up-conversion efficiency can explain the high EQE of the TCzTrz and TmCzTrz devices. In the current TADF devices, dominant light-emission mechanism is direct charge trapping by TADF emitters rather than energy transfer because of poor hole injection character of the DPEPO host. The charge trapping generates singlet and triplet excitons at a ratio of 1–3 in the TADF emitters, so the triplet exciton harvesting for singlet exciton conversion is the dominant factor for the EQE of the devices. As explained in the PL quantum yield data, the triplet to singlet conversion efficiency was relatively high in

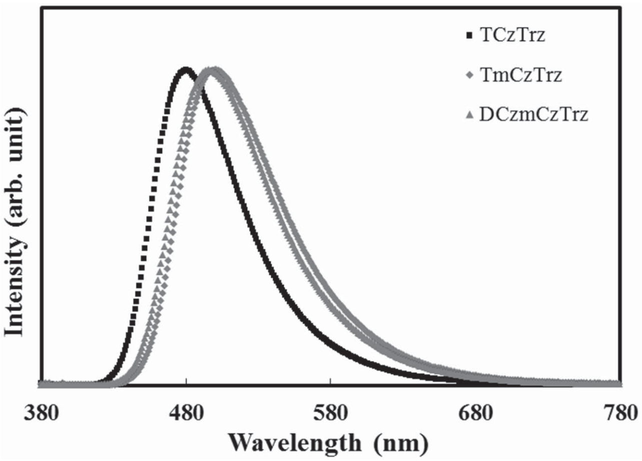

Figure 4. EL spectra of TCzTrz, TmCzTrz, and DCzmCzTrz devices. Doping concentrations of TCzTrz, TmCzTrz, and DCzmCzTrz were 40%, 30%, and 20%, respectively.

the TCzTrz and TmCzTrz, which increased the EQE in the TADF devices. The EQE calculated from the PL quantum yield of the TADF emitters is summarized in Table S2, Supporting Information, which coincided with the measured EQE values of the TADF devices. Therefore, the device performances were well correlated with the PL emission characteristics of the TADF emitters. Other parameters such as fluorescent rate constant had little effect on the device performances. From the EQE of the TADF devices, it can be concluded that the uniform dispersion of the HOMO over many donor units of the TADF emitters is critical to the device performances of the TADF emitters. High optimum doping concentration of the TADF emitters is due to the balanced hole and electron density at high doping concentration due to better hole injection by TADF emitters.

Electroluminescence (EL) spectra of the TADF devices characterized using spectroradiometer are presented in **Figure 4**. Comparison of the EL spectra of TCzTrz and DCzTrz devices revealed that the addition of more carbazole units induced bathochromic shift of the EL emission. EL peak positions of TCzTrz and DCzTrz devices were 480 and 459 nm,[10] respectively. The EL spectra of the TCzTrz, TmCzTrz, and DCzmCzTrz devices were also different and the presence of 3,6-dimethylcarbazole altered the EL peak position to long wavelength. EL peak positions of TCzTrz, TmCzTrz, and DCzmCzTrz devices were 480, 500, and 496 nm, respectively, without any other emission. Color coordinates of all TADF devices are listed in **Table 2** in addition to other device performances.

In conclusion, a molecular design approach to realize high EQE in the TADF devices by increasing the number of donor units and dispersing the HOMO evenly over the donor units was effective to obtain high PL quantum yield close to 100% and high EQE above 25% in the green and blue TADF OLEDs. The increase in the number of donor units contributed to reduce the ΔE_{ST} of the TADF emitter and uniform dispersion of the HOMO enhanced PL quantum yield and triplet to singlet conversion efficiency of the TADF emitter. Therefore, the molecular design strategy to include more donor units and distribute the HOMO uniformly would allow the development of high EQE TADF devices.

Table 2. Quantum efficiency and color coordinate of DCzTrz, TCzTrz, TmCzTrz, and DCzmCzTrz devices.

	Quantum efficiency [%]		Power efficiency [lm W^{-1}]		Color coordinate at 500 cd m^{-2}
	Maximum	500 cd m^{-2}	Maximum	500 cd m^{-2}	
DCzTrz[10]	17.8	14.9	22.4	12.7	(0.15, 0.16)
TCzTrz	25.0	16.7	42.7	18.0	(0.18, 0.33)
TmCzTrz	25.5	17.3	52.1	18.6	(0.25, 0.50)
DCzmCzTrz	21.3	14.6	42.4	16.8	(0.23, 0.46)

Experimental Section

Synthesis: Detailed synthesis of TCzTrz, TmCzTrz, and DCzmCzTrz is explained in the Supporting Information.

Device Fabrication and Measurement: This measurement method was the same as reported in previous work.[10] The device structure on indium tin oxide substrate was PEDOT:PSS (60 nm)/TAPC (20 nm)/mCP (10 nm)/DPEPO:TADF emitter (25 nm)/TSPO1 (5 nm)/TPBI (20 nm)/LiF (1 nm)/Al (200 nm). In the device structure, PEDOT:PSS, TAPC, mCP, TSPO1, and TPBI represent poly(3,4-ethylenedioxythiophene):poly(styrenesulfonate), 4,4′-cyclohexylidenebis[*N*,*N*-bis(4-methylphenyl)aniline], 1,3-bis(*N*-carbazolyl)benzene, diphenylphosphine oxide-4-(triphenylsilyl)phenyl, and 1,3,5-tris(*N*-phenylbenzimidazole-2-yl) benzene. Doping concentrations of TCzTrz, TmCzTrz, and DCzmCzTrz in the DPEPO host were 40%, 30%, and 20%, respectively, which were optimized doping concentrations in terms of EQE.

Supporting Information

Supporting Information is available from the Wiley Online Library or from the author.

Acknowledgements

This research was supported by Basic Science Research Program through the National Research Foundation of Korea (NRF) funded by the Ministry of Education, Science, and Technology (2013R1A1A2007991) and Ministry of Science, ICT, and future Planning (2013R1A2A2A01067447).

Received: April 29, 2015
Revised: June 25, 2015

---

[1] C. W. Tang, S. A. VanSlyke, *Appl. Phys. Lett.* **1986**, *48*, 183.
[2] M. A. Baldo, D. F. O'Brien, Y. You, A. Shoustikov, S. Sibley, M. E. Thompson, S. R. Forrest, *Nature* **1998**, *395*, 151.
[3] H. Uoyama, K. Goushi, K. Shizu, H. Nomura, C. Adachi, *Nature* **2012**, *492*, 234.
[4] K. Udagawa, H. Sasabe, C. Cai, J. Kido, *Adv. Mater.* **2014**, *26*, 5062.
[5] C.-W. Lee, J.-Y. Lee, *Adv. Mater.* **2013**, *25*, 5450.

[6] Y.-S. Park, S. Lee, K.-H. Kim, S.-Y. Kim, J.-H. Lee, J.-J. Kim, *Adv. Funct. Mater.* **2013**, *23*, 4914.

[7] Q. Wang, I. W. H. Oswald, X. Yang, G. Zhou, H. Jia, Q. Qiao, Y. Chen, J. Hoshikawa-Halbert, B. E. Gnade, *Adv. Mater.* **2014**, *26*, 8107.

[8] S. Hirata, Y. Sakai, K. Masui, H. Tanaka, S. Y. Lee, H. Nomura, N. Nakamura, M. Yasumatsu, H. Nakanotani, Q. Zhang, K. Shizu, H. Miyazaki, C. Adachi, *Nat. Mater.* **2015**, *14*, 330.

[9] Q. Zhang, B. Li, S. Huang, H. Nomura, H. Tanaka, C. Adachi, *Nat. Photonics* **2014**, *8*, 326.

[10] M. Kim, S. K. Jeon, S.-H. Hwang, J. Y. Lee, *Adv. Mater.* **2015**, *27*, 2515.

[11] J. Lee, K. Shizu, H. Tanaka, H. Nomura, T. Yasuda, C. Adachi, *J. Mater. Chem C.* **2013**, *1*, 4599.

[12] H. Wang, L. Xie, Q. Peng, L. Meng, Y. Wang, Y. Yi, P. Wang, *Adv. Mater.* **2014**, *26*, 5198.

[13] G. Mehes, H. Nomura, Q. Zhang, T. Nakagawa, C. Adachi, *Angew. Chem. Int. Ed.* **2012**, *51*, 11311.

[14] Q. Zhang, J. Li, K. Shizu, S. Huang, S. Hirata, H. Miyazaki, C. Adachi, *J. Am. Chem. Soc.* **2012**, *134*, 14706.

[15] Y. J. Cho, S. K. Jeon, B. D. Chin, E. Yu, J. Y. Lee, *Angew. Chem. Int. Ed.* **2015**, *54*, 5201.

[16] S. Y. Lee, T. Yasuda, H. Nomura, C. Adachi, *Appl. Phys. Lett.* **2012**, *101*, 093306.